Available online at www.sciencedirect.com
ScienceDirect
Coordination Chemistry Reviews 250 (2006) 2745–2757
COORDINATION CHEMISTRY REVIEWS
www.elsevier.com/locate/ccr

Review

A selective review on the making of coordination networks with potential semiconductive properties

Zhengtao Xu

Department of Biology and Chemistry, City University of Hong Kong, 83 Tat Chee Avenue, Kowloon, Hong Kong, China

Received 19 October 2005; accepted 28 December 2005
Available online 15 April 2006

Contents

Abstract

This paper provides a concise review of some recent developments in the synthesis and preparation of crystalline coordination networks with potential semiconductive properties. The scope is selective rather than inclusive, with special emphasis on representative compounds exhibiting generic features that could enhance electronic coupling between the metal center and the ligand π-systems, and, as a result, could point to general methods of forming semiconductive networks. The majority of systems selected herein are based on direct bonding interactions between the metal centers and polycyclic aromatic hydrocarbon (PAH) units, highlighting the importance of this class of organic molecules in the making of crystalline electronic materials. Besides the extensive efforts in ligand synthesis, new dimensions for accessing novel semiconductive systems are also derived from the design and choice of the metal center species, including simple ions (e.g., Ag^+), metal halide components (e.g., $BiCl_3$ and $BiBr_3$) and the more recently developed Lewis acid linkers with multiple binding sites [e.g., dirhodium(II) tetracarboxylate].

Keywords: Coordination networks; Semiconductive properties; Polycyclic aromatic hydrocarbon

1. Introduction

Solid state electronics is a rapidly growing field, where a major research area is to integrate organic semiconductive materials into electronic devices such as field effect transistors (FETs) and composite solar cells [1–16]. The widely studied organic semiconductors include polymeric/oligomeric systems (e.g., oligothiophenes and oligophenyls) [17–21], and fused aromatics (e.g., pentacene and hexabenzocoronene derivatives) [22–33]. Besides their inherent functional flexibility, organic semiconductors can often be dissolved (either directly or through chemical modification) in common solvents for low-temperature processing, thus offering great potential for large-area, flexible electronics applications. One major limitation of organic semiconductors, however, is the considerably lower charge carrier mobilities (as compared with the covalent inorganic systems such as Si, Ge and GaAs), which is fundamentally imposed by the weak van der Waals interactions between organic molecules. In fact, the major charge transport pathway in organic semiconductors is generally considered to be along the direction of maximum π–π orbital overlap between the organic molecules [34,35].

E-mail address: zhengtao@cityu.edu.hk.

0010-8545/$ – see front matter © 2006 Elsevier B.V. All rights reserved.
doi:10.1016/j.ccr.2005.12.031

To improve on this situation, it is especially helpful to enhance the electronic communications across the organic molecules by establishing intermolecular interactions beyond the van der Waals limit. In this regard, coordination bonds, with their intermediate strength between covalent and van der Waals interactions, could potentially provide an intermolecular linkage to overcome the van der Waals barrier of molecular semiconductors, while preserving the solution processability at the same time. Among the rapidly growing number of metal–organic coordination networks [36–40], however, conductive or semiconductive systems [38,41–48] remain relatively rare. The crux here is that the organic ligands usually are of low electroactivity, and their electronic communications with the metal centers are quite weak. For example, the widely used carboxylate groups as coordinating groups for extended networks constitute strong electronic barriers between the metal centers and the rest of the organic ligands, generally leading to insulating properties of the resultant solid state products.

Strong efforts are, nevertheless, being undertaken to access organic-based coordination semiconductive/conductive networks, mainly due to the far-reaching potential importance of the electronic properties of solid state organic-based materials. As metal–organic interaction is of crucial importance in this endeavor, we here focus on synthetic approaches that may point to new ways for overcoming the electronic barrier between the metal center and the organic ligand. Instead of being inclusive of the various crystal structures available in the literature, representative examples will be selected to illustrate the general synthetic principles. The reader is therefore encouraged to follow up on the status of the specific areas in greater detail through additional study of the literature. In contrast to the rather extensive synthetic efforts, studies on the transport mechanism and properties of these systems remain relatively unexplored. It is hoped that the current collection of potentially electroactive systems might help spur further theoretical interest as well as property studies on these comparatively unconventional materials.

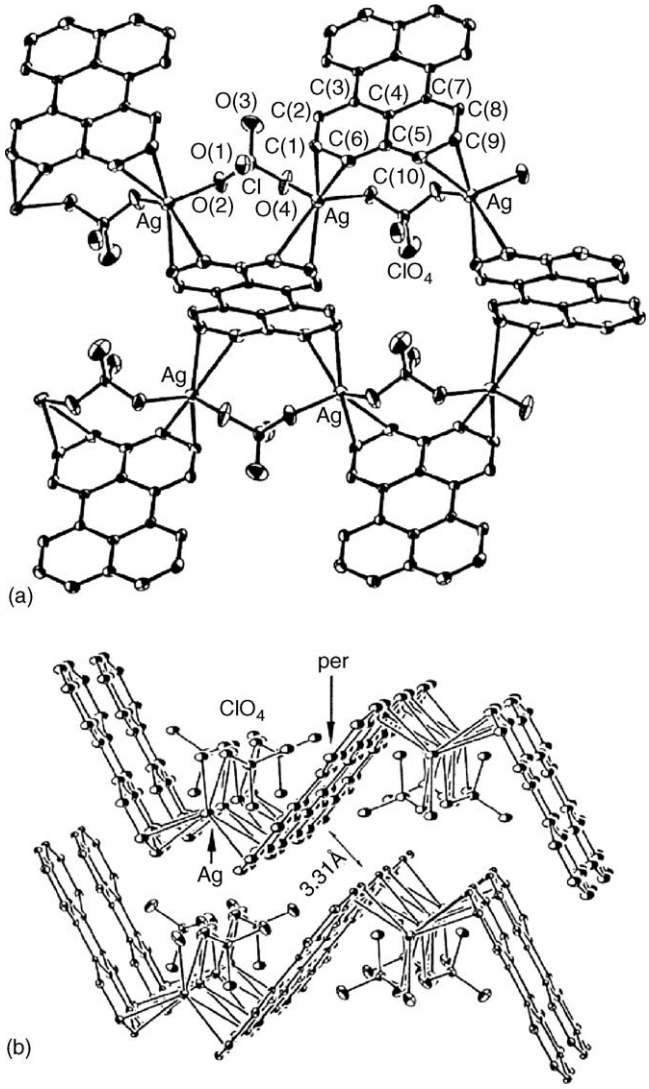

Fig. 1. (a) A portion of the infinite 2D sheet framework in $[Ag_2(per)(ClO_4)_2]$. (b) Overlapping of intersheet perylene molecules at a distance of 3.31 Å between the 2D coordination sheets (50% probability ellipsoids). Reprinted with permission from ref. [51]. Copyright 1997 American Chemical Society.

2. Cation–π networks of Ag(I) and polycyclic aromatic hydrocarbon (PAH)

Complexes of Ag(I) salts and various PAH molecules have been widely explored for potentially useful electronic properties that could arise from the π–π stacking interaction and the Ag(I)–π interactions. The Ag(I)–arene interactions often result in discrete or extended coordination networks propagating in various dimensionalities. Extensive listings of these structures can be found in the reviews by the groups of Munakata et al. and Siegel and co-workers [49,50]. The synthetic success here is largely attributed to the relatively weak and labile bonding of the Ag(I)–arene interactions, which provide reversible processes for crystallization. Weak as it is, the Ag(I)-interaction could significantly impact the electronic property of the arene moiety as well as the entire solid state, giving rise to stronger conductivity. For example, slow diffusion of *n*-hexane into a benzene solution of perylene and $AgClO_4{\cdot}H_2O$ (1:2 molar ratio, solution color is yellow) yielded orange prisms of the crystalline product $[Ag_2(per)(ClO_4)_2]$ [51]. The crystal structure of $[Ag_2(per)(ClO_4)_2]$ consists of a two-dimensional framework consisting of the metal ions bridged by the bidentate counterions and the tetra-η^2-arene groups as shown in Fig. 1a (the η^2 mode of coordination is commonly observed in these cation–π-based complexes). The four Ag–C bond distances range from 2.420(5) to 2.766(4) Å. Each perchlorate ion links two adjacent silver atoms with Ag–O distances of 2.499(5) and 2.497(5) Å, resulting in a two-dimensional W-type sandwich sheet of alternating perylene and silver(I) perchlorate groups. Such 2D sheets are further connected by the superposed intersheet aromatic π–π stackings at an average distance of 3.31 Å as illustrated in Fig. 1b. Under similar conditions, pyrene and $AgClO_4{\cdot}H_2O$ also formed yellow crystals of a 1D coordination network $[Ag_2(pyrene)(ClO_4)_2]$ (yellow) based on the cation–π interaction pyrene molecules and Ag(I) ions.

The solid samples of both $[Ag_2(per)(ClO_4)_2]$ and $[Ag_2(pyrene)(ClO_4)_2]$ display no strong ESR spectrum or

significant electrical conductivity at room temperature, indicating the lack of metal–ligand electronic communication under these conditions. However, upon irradiation for two days using a 400 W mercury lamp, the fine crystals of both complexes turned black, and exhibit ESR signals with $g = 2.003$ that is characteristic of the aromatic hydrocarbon radicals. It was proposed that the irradiation induced partial electron transfer from the aromatic donor to the silver(I) ion, forming organic radical cation and silver(0). In addition, the I_2-doped samples of both complexes also turned black and exhibited even stronger ESR spectra of cation radicals. This suggested that both perylene and pyrene could be more effectively oxidized by iodine doping than light irradiation. The I_2-doped complexes also display semiconducting behavior at ambient temperature with σ_{300} values of 1.7×10^{-5} and 4.4×10^{-5} S cm^{-1} for the pyrene and perylene-based samples, respectively.

Research along this direction has also led to a wide array of Ag(I)–arene networks [50,52], some of which contain larger aromatic systems such as coronene and rubrene [53], and displayed apparently stronger electroactivity at room temperature. The detailed conduction mechanisms or pathways remain, however, largely unexplored in these systems. It appears that theoretical studies of the band structures on these complexes may help delineate the contributions to the electronic properties from the different types of intermolecular forces such as the π–π stacking and the cation–π interactions.

The PAH-containing organosilver(I) systems as mentioned above commonly consist of distinct donor and acceptor species, with the Ag(I) ions acting as the cationic components in the charge transfer solids. By comparison, a recent Ag(I)–π network compound reported by Chen and co-workers is based on the single-component molecular species of $[Ag_2(ophen)_2]$ (Hophen = 1*H*-[1,10]phenanthrolin-2-one; see Fig. 2) [54]. The molecular complex $Ag_2(ophen)_2$ displays an intramolecular Ag(I)···Ag(I) distance of 2.801(1) Å, which is significantly shorter than the Ag···Ag separation of 2.88 Å in the metallic state, indicating a very strong Ag···Ag interaction. The solid state packing of the $Ag_2(ophen)_2$ species is based on strong off-set π–π stacking interactions with an unusually short ring-to-ring distance of ca. 3.15 Å between adjacent molecules and silver(I)–π interactions with the Ag···C contact

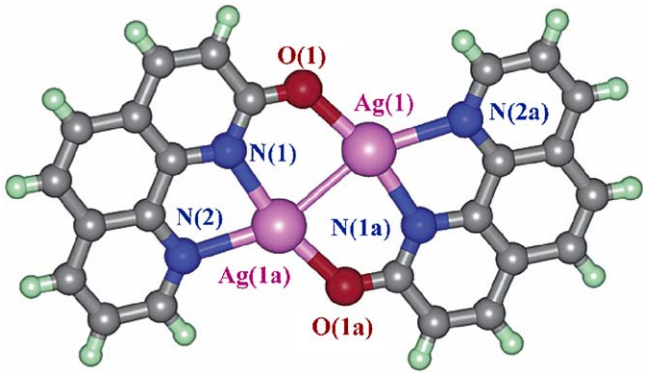

Fig. 2. A perspective view of the molecular structure of $Ag_2(ophen)_2$. Reprinted with permission from ref. [54]. Copyright 2003 American Chemical Society.

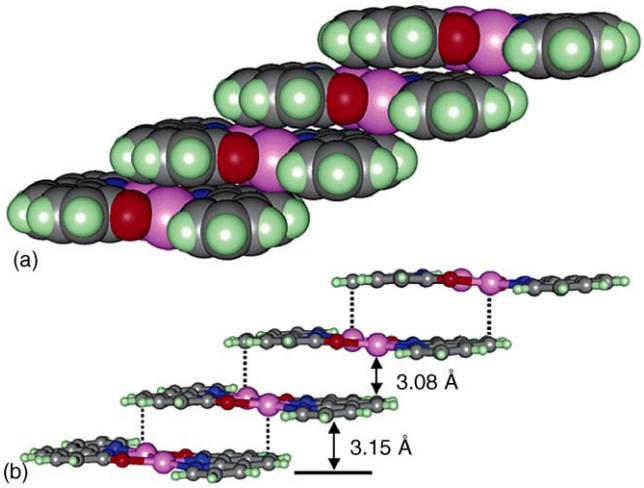

Fig. 3. Perspective views of the compact aromatic π–π stacking interactions and significant interactions between the Ag(I) ion and aromatic group in compound $Ag_2(ophen)_2$. (a) Space-filling model and (b) ball-and-stick model. Reprinted with permission from ref. [54]. Copyright 2003 American Chemical Society.

of 3.082 Å between adjacent molecules, furnishing a staircase-like one-dimensional architecture (see Fig. 3). The solid state compound is thus structurally different from the above PAH-containing organosilver(I) materials and the known conducting single-component molecular materials of transition-metal complexes with sulfur-containing π-delocalized dithiolene ligands.

Besides a room-temperature conductivity of 14 S cm^{-1}, the solid sample (neutral, not irradiated) of $[Ag_2(ophen)_2]$ exhibits a sharp ESR signal with $g = 2.00$ at room temperature, attributable to the aromatic radicals, as well as a very broad ESR signal centered approximately at $g \approx 2.05$ at 8.5 K indicating the formation of Ag(0) or Ag(II) species. It was suggested that the electron transfer takes place between adjacent molecules via the two possible pathways of Ag(I)–π and π–π interactions. Such observations imply that both the electron donor and acceptor have been combined in a single molecule of $Ag_2(ophen)_2$, highlighting its difference from the above-mentioned multicomponent organosilver(I) systems with Ag(I)–π interactions.

3. Metal halide–aromatic hydrocarbon complexes

Another group of compounds that feature significant electronic interactions between the ligand and the metal center are based on the coordination between aromatic hydrocarbon π-systems and metal halides (such as $BiBr_3$ and $BiCl_3$) components. In these systems, the metal halide components form isolated blocks or extended structures (chains or sheets), and the Bi^{3+} centers interact with (usually in the face-on mode) the organic π-systems to cause substantial charge transfer phenomena. Of particular interest to semiconductive properties are those with extended structures of delocalized electronic systems, which could potentially enhance charge carrier transport throughout the solid state. The extended structure can be realized by means of the inorganic chains or isolated fragments being integrated into higher-dimensional structures

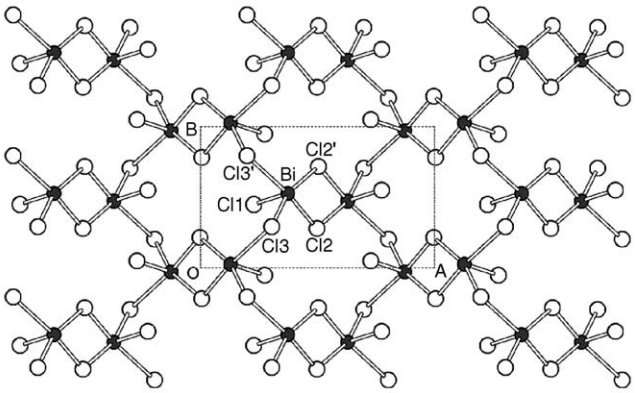

Fig. 4. The $BiCl_3$ network in the crystal structure of $2BiCl_3$·pyrene. Bond distances: Bi–Cl1, 2.44(1) Å; Bi–Cl2, 2.51(1) Å; Bi–Cl3, 2.51(1) Å; Bi–Cl2′, 3.15(1) Å; Bi–Cl3′, 3.35(1) Å.

through the coordination bonds with the π-electron systems from the organic ligand.

For example, mixing a *p*-xylene solution of $BiCl_3$ and pyrene led to the formation of the complex $2BiCl_3$·pyrene [55]. The single crystal structure features two pyramidal $BiCl_3$ units interacting with one crystallographically centrosymmetric pyrene molecule (Figs. 4 and 5). The bridging Cl atoms (e.g., Cl2 and Cl3; see Fig. 4) connect the $BiCl_3$ units in a 2D network that is further interconnected by the pyrene molecules. The interaction between the Bi^{3+} centers and the pyrene molecules is characterized by short Bi···C distances such as 3.25, 3.27 and 3.39 Å (van der Waals distance between C and Bi >3.7 Å [56]), as is shown in Fig. 5. Counting both the Bi–Cl and Bi–C coordination interactions, one can therefore consider the current structure a 3D coordination network. The red-purple color of the crystalline product, in contrast with the almost colorless starting materials of pyrene and $BiCl_3$, might be considered as significant charge transfer (CT) between the pyrene and $BiCl_3$ components within the extended structure.

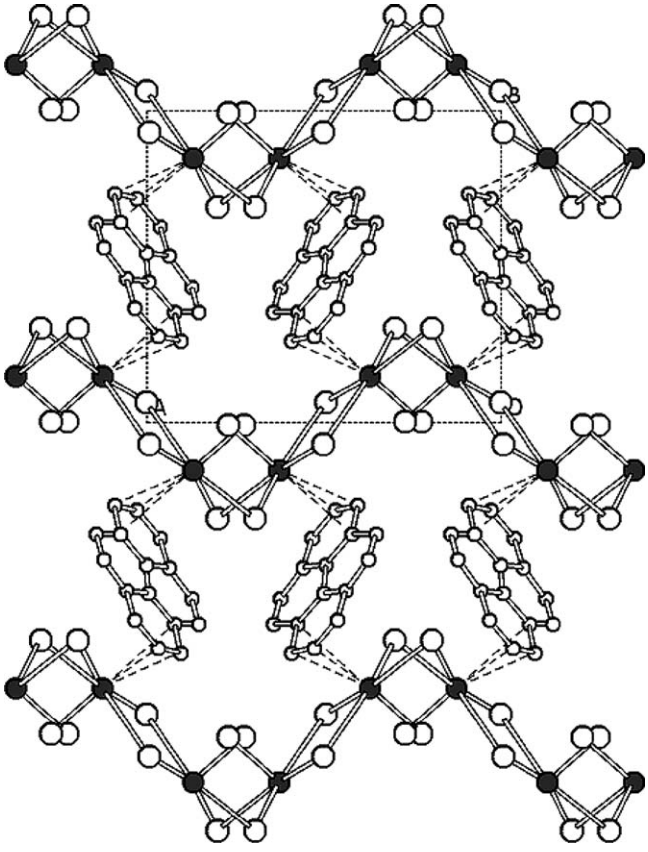

Fig. 5. Projection of the crystal structure of $2BiCl_3$·pyrene along the *c* axis. Dotted lines designate Bi···C contacts shorter than 3.5 Å.

Along a similar line, other aromatic molecules that have been incorporated into CT complex with bismuth halides include benzene [57], perylene [58], fluorene [59], fluoranthene [59] and several paracyclophanes [60,61]. In the complex of C_6H_6·$BiCl_3$, the $BiCl_3$ components also form into 2D networks. The bismuth–π-system interactions are less interconnecting than in the above $2BiCl_3$·pyrene, with each benzene molecule confined to one Bi^{3+} center in the η^6 mode (the overall coordination network therefore remains 2D). By comparison, the larger perylene molecule interacts with $BiBr_3$ to form the complex (perylene)$_3$ [Bi_4Br_{12}] featuring isolated tetrameric units of Bi_4Br_{12} embedded in a matrix of the organic molecules, with no extended coordination net formed as a result. A summary of the CT property for some of these complexes is available [59], which indicated a linear correlation (with slope of 1) between the charge transfer band energies $E_{c,t}$ and the ionization potentials of the electron donors, suggesting large-size, easily polarizable organic π-systems tend to generate smaller electronic band gaps in the solid state complexes.

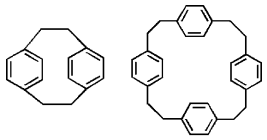

CP1 CP2

Another interesting direction is represented by the CT complexes based on metal halides (e.g., $BiBr_3$) and cyclophanes such as [2.2]-paracyclophane (CP1) [60] and the larger congener [2.2.2.2]-paracyclophane (CP2) [61], in which the multiple aryl groups of the cyclophane molecule could potentially interact with more metal centers and enhance the dimensionality of the resultant coordination networks. In the complex CP2·$2BiBr_3$·C_7H_8 (C_7H_8 is toluene), for example, the $BiBr_3$ component formed into a chain based on the edge-sharing of the pyramidal $BiBr_5$ units (Fig. 6), which was integrated into a 2D structure via the coordination between the Bi(III) center and the aromatic rings from the CP2 molecules. Similar structural motifs are also observed in compound CP1·$2BiBr_3$ with regards the $BiBr_3$ chain and the overall connectivity of the coordination network. With regards the construction of semiconductive networks, one drawback of the current cyclophane-based hybrid systems stems from the saturated and non-conjugating ethylene ($–CH_2CH_2–$) groups separating the aryl rings and blocking the electronic communication between the π-electron systems. The imbedded idea of introducing multiple aryl groups into the ligand for achieving higher-dimensional networks is, however, an

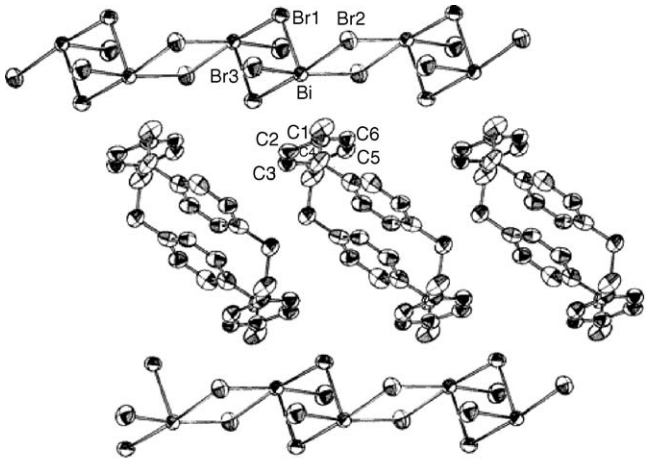

Fig. 6. A perspective view of the structure of $CP2{\cdot}2BiBr_3{\cdot}C_7H_8$ with thermal ellipsoids at 50% probability level (toluene molecules are omitted). The carbon atoms of the benzoid ring in close contact with the Bi^{3+} center are labeled. Bond distances: Bi–C1, 3.31(2) Å; Bi–C2, 3.40(1) Å; Bi–C3, 3.49(1) Å; Bi–C4, 3.56(2) Å; Bi–C5, 3.42(2) Å; Bi–C6, 3.27(2) Å. Reprinted with permission from ref. [61]. Copyright 1998 American Chemical Society.

interesting one, especially when effective conjugation between the aryl units could be maintained throughout the molecule.

4. Networks from dirhodium tetracarboxylate and polycyclic aromatic hydrocarbons

Recently, Cotton et al. reported a class of coordination polymers based on dirhodium(II) tetracarboxylate [e.g., $Rh_2(O_2CCF_3)_4$] and various PAH molecules [62], in which the crystal structures feature potentially effective interaction between the metal centers and the organic molecules. In these systems, the dirhodium agent contains two sites of strong Lewis acidity rigidly oriented in space, effectively linking the donor PAH molecules into extended polymeric structures. Notably, a dirhodium reagent such as $Rh_2(O_2CCF_3)_4$ is volatile, subliming rapidly at moderate temperatures (ca. 250 °C), and thus reactions can be conducted by sublimation–deposition procedures from the gas phase (i.e., in the absence of solvent). Using this solventless approach, a series of PAH/$Rh_2(O_2CCF_3)_4$ complexes with isolated, 1D and 2D network structures has been prepared, and their crystal structures determined by single crystal X-ray diffraction. For illustration, the structures of the 1D pyrene-based and the 2D triphenylene-based networks are presented in Figs. 7 and 8, respectively. In these structures, each rhodium site is usually bonded to two contiguous carbon atoms (i.e., a C–C bond, in the η^2 mode) on the exterior of the PAH molecules. Hückle calculations were performed on the corresponding molecules and indicated that the most electron-rich sites are usually bound to the rhodium sites. Although no solid state electronic band gap data are available for these compounds, the short Rh···C distances (generally between 2.4 and 2.7 Å), as well as the varying degree of coloring of the crystals, suggest that effective donor–acceptor electronic interaction is possible in these extended solid state products.

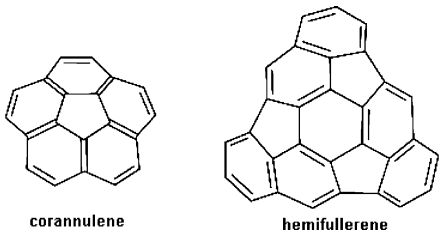

More recently, this area of chemistry has been expanded to include non-planar, bowl-shaped geodesic polyarenes such as corannulene ($C_{20}H_{10}$) and hemifullerene [63–65]. Based on the effective solvent-free synthetic approach, a number of extended organometallic networks were crystallized and characterized by X-ray studies. Such studies were primarily aimed to probe the reactivity of the π-systems of the bowl-shaped arenes with regards the convex or concave reactivity difference. It was of interest to note that the concave face appeared to react quite readily with the dirhodium reagent $Rh_2(O_2CCF_3)_4$. For example, a dark-green adduct $[Rh_2(O_2CCF_3)_4]_3{\cdot}(C_{20}H_{10})_2]$ was obtained

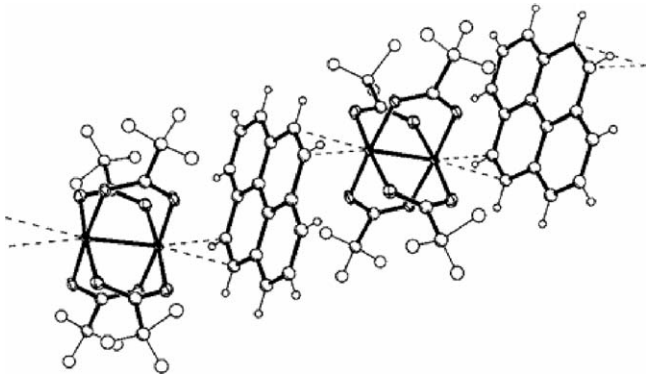

Fig. 7. The alternating arrangement of $Rh_2(O_2CCF_3)_4$ and pyrene molecules in the 1D chain structure of monoadduct of $[Rh_2(O_2CCF_3)_4]{\cdot}$pyrene. Rhodium and oxygen atoms are represented by thermal ellipsoids at the 40% probability level. Carbon, fluorine and hydrogen atoms are shown as spheres of arbitrary radii. Only one orientation of the disordered CF_3 groups is depicted. The shortest Rh–C_{arene} contacts [2.578(3) Å] are drawn by dashed lines. Similar conventions remain in Fig. 8. Reprinted with permission from ref. [62]. Copyright 2001 American Chemical Society.

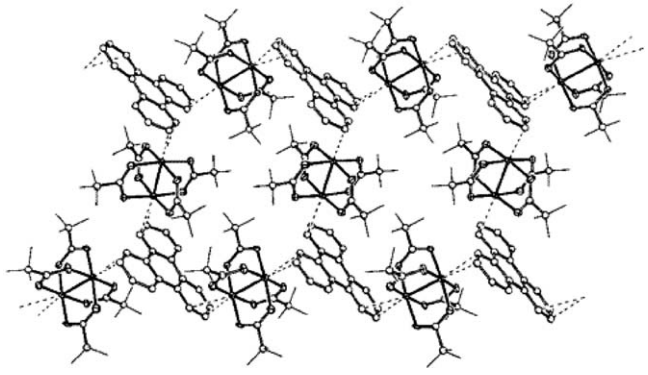

Fig. 8. The 2D coordination network in the crystal structure of $\{[Rh_2(O_2CCF_3)_4]_3{\cdot}(C_{18}H_{12})_2\}$ (with $C_{18}H_{12}$ designating one triphenylene molecule). Hydrogen atoms and fluorine atoms of CF_3 groups are omitted for clarity. Shortest Rh–C_{arene} contacts (dashed lines) are between 2.56(2) and 2.73(2) Å. Reprinted with permission from ref. [62]. Copyright 2001 American Chemical Society.

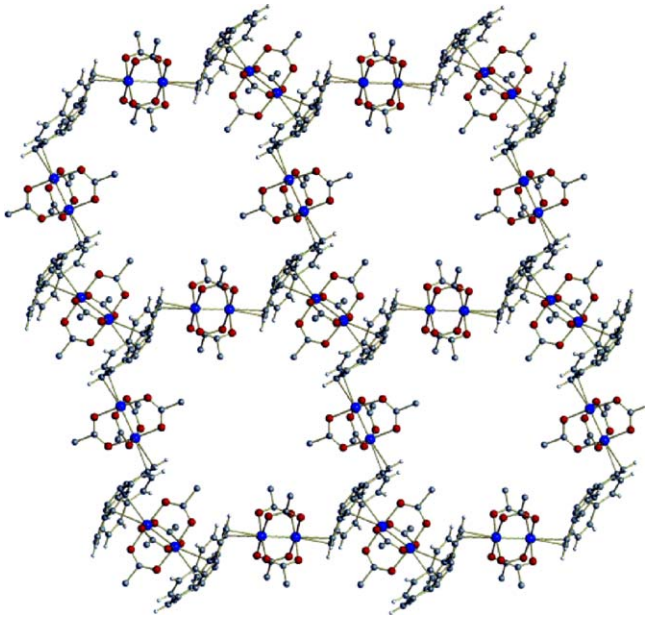

Fig. 9. A fragment of a 2D infinite layer in $[Rh_2(O_2CCF_3)_4]_3{\cdot}(C_{20}H_{10})_2$; Rh blue, O red, C gray, H light gray; fluorine atoms are omitted for clarity. Ref. [63]—reproduced by permission of Wiley–VCH Verlag GmbH. (For interpretation of the references to color in this figure legend, the reader is referred to the web version of the article.)

in yields of 30–35% in a reaction where an excess of the dimetal complex (Rh_2:$C_{20}H_{10} \approx 3$:1) was used [63]. As is typical for analogous donor–acceptor adducts with planar PAHs, the product is relatively stable in air at room temperature but is sensitive to moisture. X-ray diffraction studies of the crystals of $[Rh_2(O_2CCF_3)_4]_3{\cdot}(C_{20}H_{10})_2]$ revealed two unique local bonding motifs of weak η^2 coordination, which has an infinite 2D layered network consisting of giant hexagonal cells built of six dimetal units and six corannulene molecules (Fig. 9). Each corannulene molecule is coordinated to three dimetal units: two from the convex side and one from the concave side (Fig. 9). All three linear dirhodium units use both axial positions for coordination, with each rhodium center binding two carbon atoms of a corannulene (η^2 coordination mode). For the three crystallographically independent rhodium atoms in the asymmetric unit (Rh1, Rh2 and Rh3, with Rh1 and Rh3 bonded to the convex side and Rh2 the concave side), the Rh–C bond lengths are averaged to 2.636(3), 2.570(3) and 2.548(3) Å, respectively, with the differences between the two Rh–C bonds for each rhodium atom being 0.279, 0.010 and 0.141 Å, respectively.

5. Ligands with more distinct coordinating characters

So far we have covered systems based on metal centers directly coordinating to hydrocarbon π-electron systems. Although such direct (face-on) cation–π interactions are well-poised to provide electronic coupling between the metal center and the organic ligand, the π-electrons of the aromatic systems are usually quite weak in their coordinating ability, especially in comparison with the more distinct coordination sites with well-defined lone-pair electrons (such as sulfur, nitrogen and phosphorus atoms). In addition, the bonding directionality of the aromatic π-system is quite diffuse, posing more difficulty in correlating the ligand geometry with the connectivity of the solid state network. In view of these issues, it is pertinent to take note of electroactive π-systems (such as tetrathiafulvalene, TTF) that are equipped with chelating sites such as the organylthio [43–45] and phosphine [66–69] groups, as such ligands could potentially further enhance the bonding and electronic interaction between the metal center and the organic ligands.

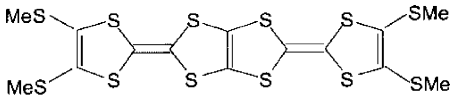

TTM-TTP

A successful way of connecting these TTF-based ligands into extended coordination frameworks is through the relatively inert interaction with Ag(I) or Cu(I) species [43–45,70]. For example, slow diffusion of hexane into an acetonitrile/benzene solution of $AgCF_3SO_3$ and the ligand TTM-TTP resulted in an orange needle-like crystalline product $Ag(TTM\text{-}TTP)(CF_3SO_3)$ comprised of 1D coordination network (see Fig. 10) [43]. Besides the Ag(I)–S coordination bonds, extensive intermolecular S···S contacts also exists in the face-to-face fashion and side-to-side modes, providing additional interactions across the individual chain. Moreover, black solid with the composition $[Ag(TTM\text{-}TTP)(CF_3SO_3)](I_3)_{0.29}$ can be obtained by depositing I_2 vapor onto a ground sample of $Ag(TTM\text{-}TTP)(CF_3SO_3)$. The electrical conductivities of the free TTM-TTP, complex $Ag(TTM\text{-}TTP)(CF_3SO_3)$ and the iodine-doped sample were measured by the conventional two-probe technique at room temperature. The free TTM-TTP is an insulator ($\sigma_{25\,^\circ C} < 10^{-12}\,S\,cm^{-1}$), while complex $Ag(TTM\text{-}TTP)(CF_3SO_3)$ and the iodine-doped sample show different conductivities with $\sigma_{25\,^\circ C}$ of 7.1×10^{-6} and $0.85\,S\,cm^{-1}$, respectively. Although the conduction pathway was ascribed to the ligand–ligand interactions of $TTM\text{-}TTP^{\bullet+}$/TTM-TTP or $TTM\text{-}TTP^{\bullet+}/TTM\text{-}TTP^{\bullet+}$, the role of the Ag(I)–S coordination bonds in the conductivity properties remains an interesting topic to explore. An intense well-resolved ESR resonance was observed with g values of 2.007 and 2.004, which can be ascribed to the $TTM\text{-}TTP^{\bullet+}$ cation radicals for complex $[Ag(TTM\text{-}TTP)(CF_3SO_3)]$ and the iodine-doped sample, respectively. The spin density for the TTM-TTP cation radicals was measured with the diphenylpicrylhydrazyl (DPPH) as a standard, being 15.8% for $[Ag(TTM\text{-}TTP)(CF_3SO_3)]$ and 87.0% for the doped sample, respectively. It is noted that the

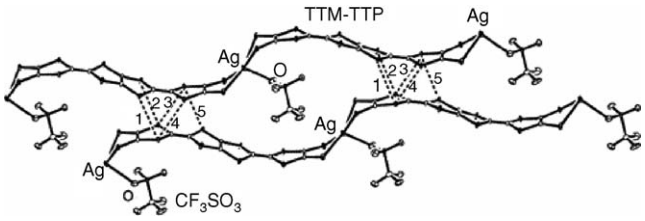

Fig. 10. Side view of two 1D coordination nets in $Ag(TTM\text{-}TTP)(CF_3SO_3)$ with face-to-face S···S contacts (1, 3.68 Å; 2, 3.71 Å; 3, 3.55 Å; 4, 3.68 Å; 5, 3.66 Å). The methyl groups are omitted. Reprinted with permission from ref. [43]. Copyright 2001 American Chemical Society.

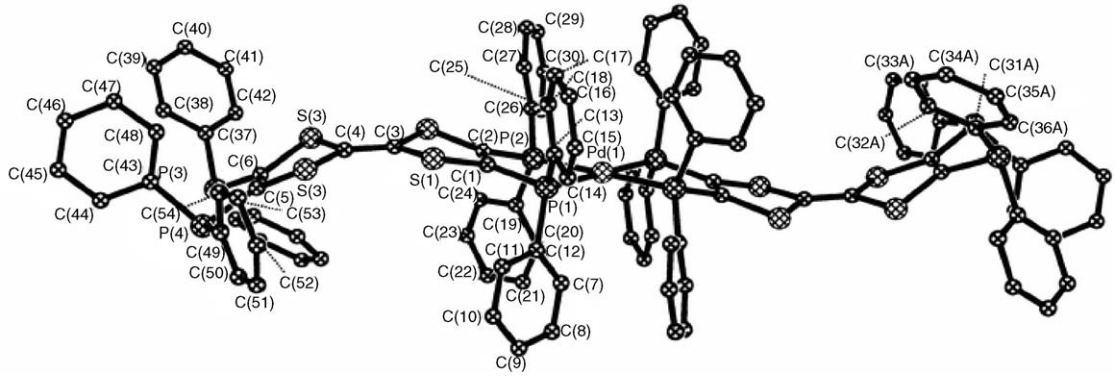

Fig. 11. Labeled diagram of the complex cation Pd(**P4**)$_2^{2+}$ in the crystal structure of compound [Pd(**P4**)$_2$][BF_4]$_2$·CH_2Cl_2. Ref. [66]—reproduced by permission of The Royal Society of Chemistry.

high conductivity of the doped sample is attributable to its high spin density.

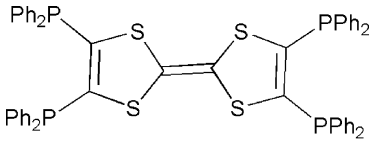

P4

Given the strong redox activity of the TTF-based ligands, networks based on their coordination with more reactive metal species (e.g., open-shell transition metal ions) could give rise to strong metal–ligand electronic coupling, generating potentially rich combinations of physical properties of conductivity and magnetism. Attempts to incorporate more electroactive metal ions such as Pd^{2+}, Pt^{2+} or the larger $Re_2Cl_8^{2-}$ have, however, generally resulted in isolated species, instead of extended networks, apparently due to the overly irreversible chelation interaction between the TTF-ligands and the selected metal ion species [45,66,68,71,72]. For example, a reaction between [Pd(NCMe)$_4$][BF_4]$_2$ and the tetrathiafulvalene-based phosphine ligand **P4** in the presence of CH_2Cl_2 resulted in the crystallization of the brown compound [Pd(**P4**)$_2$][BF_4]$_2$·CH_2Cl_2, which contains the square planar cation Pd^{2+} being coordinated by two **P4** ligands (see Fig. 11) [66]. Electrochemical studies indicate that the TTF redox centers on the individual complex ions of Pd(**P4**)$_2^{2+}$ are electronically isolated in this and other related compounds reported in the same paper. The polymeric products are presumably too insoluble to be crystallized under the experimental conditions. In spite of the current difficulties in obtaining extended crystalline structures, the numerous metal complexes of tetrathiafulvalene-based ligands thus obtained have greatly expanded the understanding of the chemistry and physical properties of the tetrathiafulvalene-based materials, paving way for exploring the electronic and magnetic properties in more advanced systems.

6. Coordination networks of large aromatic thioether ligands and bismuth halides

Before touching upon other semiconductive networks in this section, let us briefly introduce the extensive pioneering work of Reid and co-workers regarding the coordination complexes based on Group 15 trihalides (MX_3, M = As, Sb, Bi; X = Cl, Br, I) and chalcogeno-ether ligands. In these complexes, the inorganic halide components usually formed into isolated blocks (e.g., dimeric or tertrameric units) or infinite chains, which are further connected into organic–inorganic networks of various dimensionalities by means of the coordination with monodentate or multidentate chalcogeno-ether ligands [73–80]. For example, red crystals of the complex [$BiBr_3$(PhTeMe)] were obtained by slow evaporation from an MeCN solution of $BiBr_3$ that was layered with an equimolar solution of the ligand methyltellurobenzene PhTeMe in CH_2Cl_2 [80]. The crystal structure showed (see Fig. 12) a planar asymmetric $Br_2Bi(\mu\text{-}Br)_2BiBr_2$ dimer unit with one PhTeMe ligand coordinated apically to each Bi and occupying mutually *anti* positions. Br(3) and Br(3b) form additional long contacts (3.16 Å) via the open Bi vertex and hence link adjacent units to give an infinite chain of Bi_2Br_6(PhTeMe)$_2$ dimers in a step-like arrangement (Fig. 12b). Although electronic structure or property studies on this type of coordination networks have not been reported, the idea of using intervening metal halide fragments (in lieu of individual metal ions) to connect organic ligands into extended networks points to interesting possibilities for making hybrid semiconductors, especially when effective electronic communication between the organic ligands and metal halide components could be established.

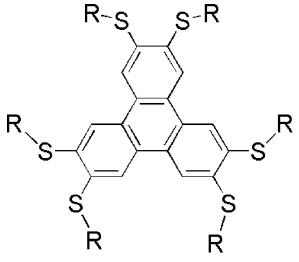

R = —CH_3 HMTT
R = —C_2H_5 HETT
R = —$CH(CH_3)_2$ HiPTT

Such possibilities are illustrated by a class of recently reported semiconductive networks that features rather promising

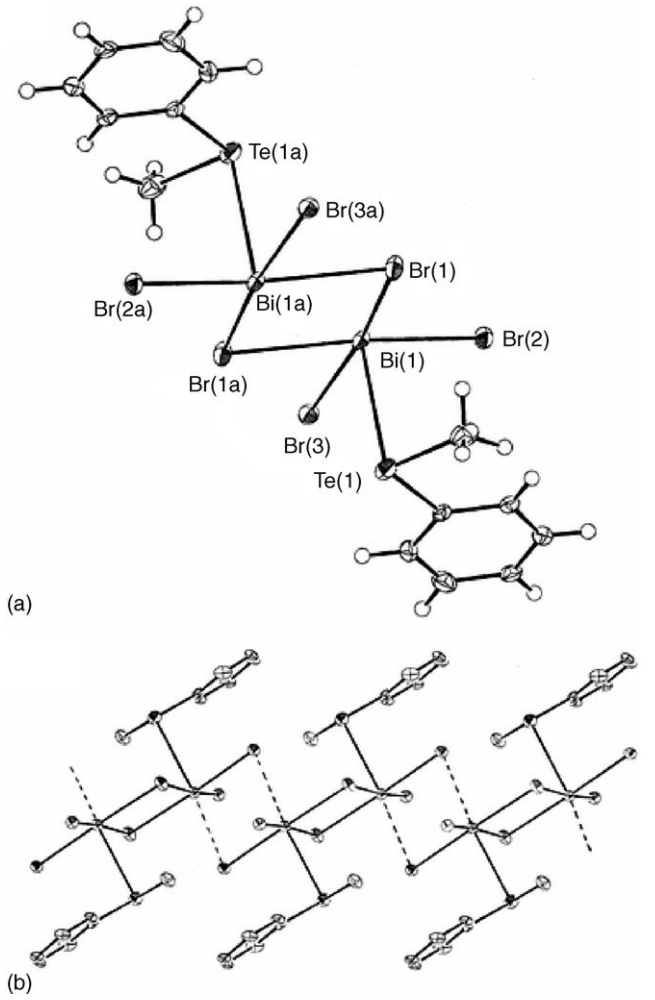

Fig. 12. (a) View of the crystal structure of the dimeric unit in [$BiBr_3$(PhTeMe)] with numbering scheme adopted. Ellipsoids are shown at the 40% probability level. Selected bond lengths (Å): Bi(1)–Te(1) 3.0533(7), Bi(1)–Br(1) 2.8291(10), Bi(1)–Br(1a) 3.0810(10), Bi(1)–Br(2) 2.6497(9) and Bi(1)–Br(3) 2.8570(9). (b) View of [$BiBr_3$(PhTeMe)] showing the interdimer Bi···Br contacts (3.16 Å) generating the infinite chains. Ref. [80]—reproduced by permission of The Royal Society of Chemistry.

properties of effective metal–ligand interaction, solution processability and air stability [81,82]. The reported approach strived to integrate the various design elements of the previous methods, in order to construct functional semiconductive networks based upon the interaction between metal halide component and large aromatic molecules containing multiple chelating thioether groups, such as the 2,3,6,7,10,11-hexakis(alkylthio)triphenylene molecules (alkyl: methyl, ethyl and isopropyl; corresponding abbreviations for the molecules: HMTT, HETT and HiPTT). It was found that mildly oxidizing metal halide fragments such as bismuth(III) bromide are particularly suitable for linking the organic ligands into semiconductive networks, while providing effective electronic coupling between the organic π-system and the metal center.

Fig. 13 shows the crystal structures of a series of coordination networks based on HRTT molecules and $BiBr_3$ (or $BiCl_3$) components (for comparison, the crystal structure of the HMTT compound is also shown). In compound HMTT $2BiBr_3$, the 1D chains of $BiBr_3$ component are connected by the HMTT ligands (two pairs of sulfur atoms from the HMTT molecule coordinate to the Bi^{3+} center, while the other pair stays unbonded), resulting in a 2D coordination network. In compounds HMTT·$BiBr_3$ and HMTT·$BiCl_3$, the HMTT molecule only engages one pair of its sulfur atoms in coordination with the bismuth halide chains, and the overall coordination network is 1D. In compounds HETT·$2BiBr_3$ and HiPTT·$2BiBr_3$, the dimensionalities of the coordination networks can be considered quasi-1D and 0D, respectively. Overall, enlarging the side group from methyl (i.e., HMTT) to ethyl (i.e., HETT) and to isopropyl (i.e., HiPTT) groups effectively reduces the dimensionality of the bismuth halide components (and consequently the dimensionality of the overall coordination framework).

Table 1
Structure–property relations for HMTT·$2BiBr_3$, HMTT·$BiBr_3$, HMTT·$BiCl_3$, HETT·$2BiBr_3$, HiPTT·$2BiBr_3$ and HMTT

Compounds	Network dimensionality	Band gap (eV)
HMTT·$2BiBr_3$	2D	1.64
HMTT·$BiBr_3$	1D	1.75
HMTT·$BiCl_3$	1D	1.82
HETT·$2BiBr_3$	Quasi-1D	1.97
HiPTT·$2BiBr_3$	0D	2.18
HMTT	0D	2.98

To probe the relations between crystal structures and electronic properties, the diffuse reflectance spectra of these samples were systematically studied for measuring the electronic band gaps. As is shown in Fig. 14 and Table 1, all the hybrid compounds (2.3–1.8 eV, colors steadily transitioning from the orange of HiPTT·$2BiBr_3$ to the dark red of HMTT·$2BiBr_3$) show band gaps substantially smaller than those of the HMTT compound (3.1 eV, colorless) and the $BiBr_3$ solid (2.7 eV, colorless), indicating significant electronic interaction between the organic ligands and the inorganic components.

More interestingly, as the dimensionality of the coordination network decreases, the electronic band gap consistently increases, suggesting that the Bi–S and Bi–X coordination bonds have overtaken the π–π interaction between the organic molecules as the major determinant of the solid state electronic properties. In other words, significant electronic interactions have been installed between the organic π-systems and the intervening BiX_3 moieties, which effectively integrate the individual molecules into hybrid semiconductive networks. Although charge carrier mobility measurement on these hybrid semiconductors still needs to be done, charge transport in these hybrid systems might be expected to follow the pathways of the coordination framework (as well as the π–π stacking directions). Compared with the typical molecular semiconductors, the stronger intermolecular connections (i.e., the Bi–S and Bi–X coordination bonds) in these hybrid networks might thus lead to potentially higher charge carrier mobilities. In addition, these hybrid semiconductors are air-stable, and show strong promise for low-cost processing. For example, they can be dissolved in

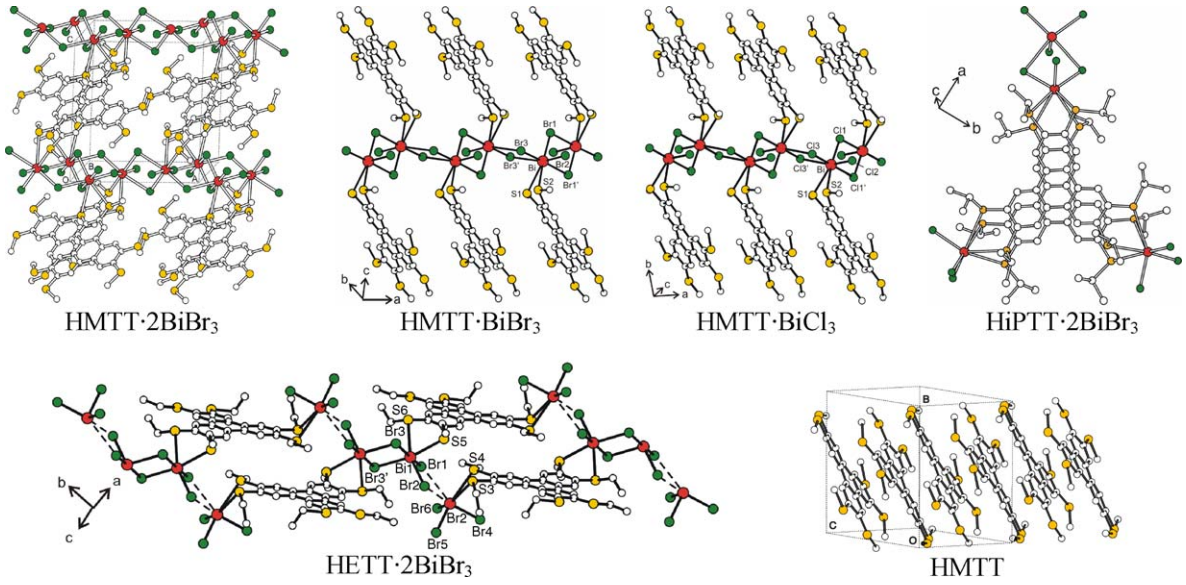

Fig. 13. Single crystal structures of a series of coordination networks based on HRTT molecules and $BiBr_3$/$BiCl_3$ [i.e., compounds HMTT·2$BiBr_3$, HMTT·$BiBr_3$, HMTT·$BiCl_3$, HETT·2$BiBr_3$ and HiPTT·2$BiBr_3$], together with the crystal structure of HMTT. Large red sphere: Bi; medium green: Cl or Br; medium yellow: S; small white: C. Dashed lines in HETT·2$BiBr_3$ indicate elongated Bi–Br bonds, reducing the dimensionality from 1D to quasi-1D. Reprinted with permission from ref. [82]. Copyright 2005 American Chemical Society. (For interpretation of the references to color in this figure legend, the reader is referred to the web version of the article.)

heated solvents such as 1,2-dichlorobenzene or benzene, and then deposited directly from the solutions in practically quantitative yields.

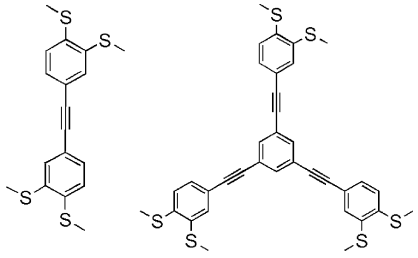

Building on this discovery, similar synthetic strategy has also been extended to phenylalkyne-based ligands such as 3,3′,4,4′-tetrakis(methylthio)tolan (TMT) and 1,3,5-tris{[3,4-bis(methylthio)phenyl]ethynyl}benzene (TBMPEB). Molecule TMT reacts with $BiBr_3$ to form a 2D semiconductive coordination network (TMT·2$BiBr_3$), which consists of infinite chains of the $BiBr_3$ component cross-linked by TMT through the chelation between the 1,2-bis(methylthio) groups and the Bi(III) centers (Fig. 15) [83]. Notice that the $BiBr_3$ chains in TMT·2$BiBr_3$ share the same connectivity as the ones in compounds HMTT·$BiBr_3$ and HMTT·$BiCl_3$, as well as in the above-mentioned $Bi_2Br_6(PhTeMe)_2$ and CP2·2$BiBr_3$·C_7H_8. Molecule TBMPEB reacts with $BiBr_3$ to form a 1D semiconductive coordination network (TBMPEB·2$BiBr_3$), which features discrete tetrameric Bi_4Br_{12} units linked by the thioether groups from TBMPEB [Fig. 16; only two of the three 1,2-bis(methylthio) groups from each TBMPEB molecule are bonded to the Bi(III) centers]. Diffuse reflectance spectra of both TMT·2$BiBr_3$ and TBMPEB·2$BiBr_3$ feature strong optical absorptions at energy levels (Fig. 17; around 2.1 eV) significantly lower than those of the corresponding molecular solids of TMT, TBMPEB and $BiBr_3$ (all above 2.5 eV), indicating significant electronic interaction between the organic π-electron systems and the $BiBr_3$ components. In addition, both TMT·2$BiBr_3$ and TBMPEB·2$BiBr_3$ readily form in high yields and are stable to air, providing advantages for further studies as potentially applicable semiconductive materials.

At this point, it may be relevant to comment on the bismuth(III) halide component with regard to the potential advantages that it provides in forming the networks of the above sections. First, Bi(III) is slightly oxidative and may serve as

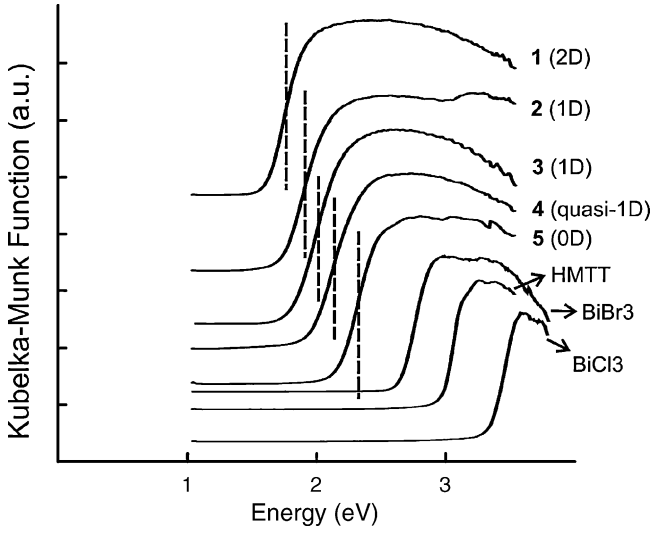

Fig. 14. Room-temperature optical absorption spectra for solid samples of HMTT·2$BiBr_3$ (**1**), HMTT·$BiBr_3$ (**2**), HMTT·$BiCl_3$ (**3**), HETT·2$BiBr_3$ (**4**), HiPTT·2$BiBr_3$ (**5**), HMTT, $BiCl_3$ and $BiBr_3$. Dotted lines highlight the relative positions of the absorption edges.

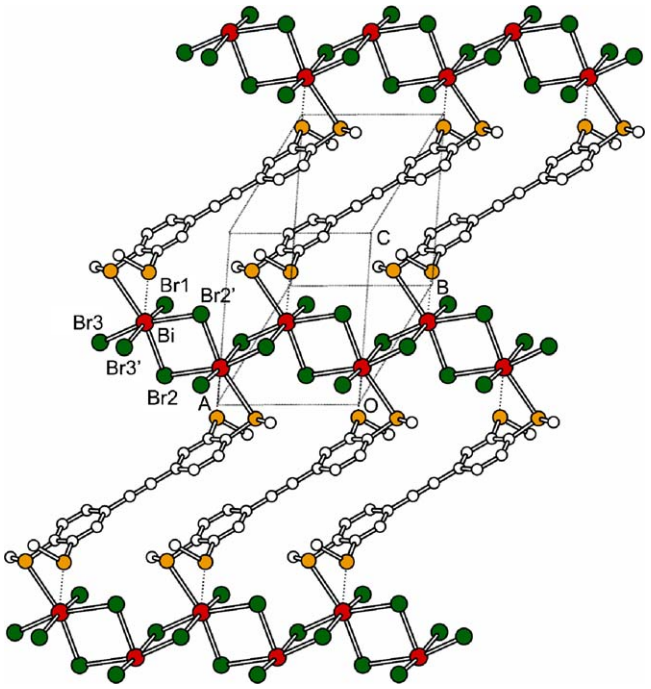

Fig. 15. A 2D coordination network in TMT·2BiBr$_3$. Large red sphere: Bi; medium green: Br; medium yellow: S; small white: C. Dotted lines show the longer Bi–S distance (3.486 Å). Reprinted with permission from ref. [83]. Copyright 2005 American Chemical Society. (For interpretation of the references to color in this figure legend, the reader is referred to the web version of the article.)

an electron acceptor for the aromatic π-system, thus facilitating charge transfer between the organic and inorganic components. Second, as a heavy p-block element, Bi(III) tends to display a high coordination number, especially in halide compounds, where secondary Bi–X (X: halogen atoms) interactions [84,85] often furnish a seven-fold (or higher) coordination sphere around the Bi center. Such a high coordination number promotes the formation of extended networks in the solid state, generating more extensive interconnections across the organic molecules. In addition, hybrid networks involving metal–halogen bonds [86–99] tend to be more soluble in organic solvents than other inorganic compounds such as chalcogenides, and can facilitate the crystallization process as well as maintain processability [96–99] in organic solvents.

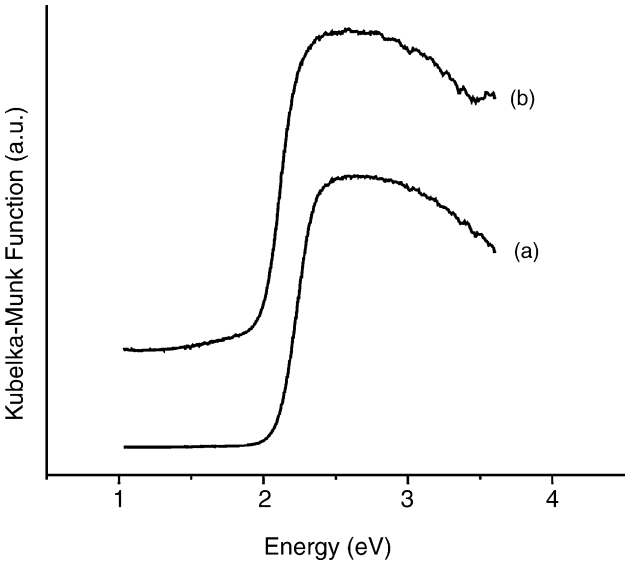

Fig. 17. Room-temperature optical absorption spectra for solid samples of: (a) TMT·2BiBr$_3$ and (b) TBMPEB·2BiBr$_3$. Reprinted with permission from ref. [83]. Copyright 2005 American Chemical Society.

7. Other systems of semiconductive networks

Building on the previous research on porous chalcogenide frameworks, Feng and Bu recently reported a series of coordination networks in which composite chalcogenide nanoclusters were linked by organic ligands such as 1,2,4,5-tetra(4-pyridyl)benzene and different types of bipyridines [100–102]. Due to the inherent electroactivity of the chalcogenide clusters and the modifiable organic ligands, a wide range of coordination networks with potential semiconductivity could likely be derived from this synthetic approach. At this stage, it appears that further studies on the electronic interaction between the cluster moiety and the organic ligand are still needed, as such interaction would be crucial for establishing effective semiconductive transport throughout the networks.

A number of other semiconductive coordination nets have recently been reviewed by Janiak [38], including the 1D coordination polymers constructed from metalloporphyrins axially linked by ditopic ligands such as pyrazine and 4,4′-bipyridine [41,103], networks based on Ag···Ag contacts [104,105] and the

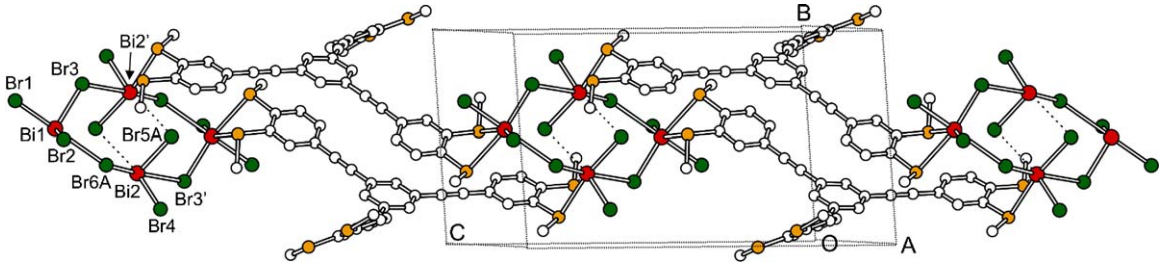

Fig. 16. The 1D coordination network in the crystal structure of TBMPEB·2BiBr$_3$. Large red sphere: Bi; medium green: Br; medium yellow: S; small white: C. Elongated Bi–Br bonds are shown in dotted lines. Selected bond lengths: Bi1–Br1, 2.6212(7) Å; Bi1–Br2, 2.6784(8) Å; Bi1–Br3, 2.7575(9) Å; Bi1–Br6A, 3.283(2) Å; Bi2–Br6A, 2.538(2) Å; Bi2–Br4, 2.6207(7) Å; Bi2–Br3′, 3.097(1) Å; Bi2–Br5A, 2.784(2) Å; Bi2′–Br5A, 3.301(2) Å (disordering of Br5A and Br6A is not shown). Reprinted with permission from ref. [83]. Copyright 2005 American Chemical Society. (For interpretation of the references to color in this figure legend, the reader is referred to the web version of the article.)

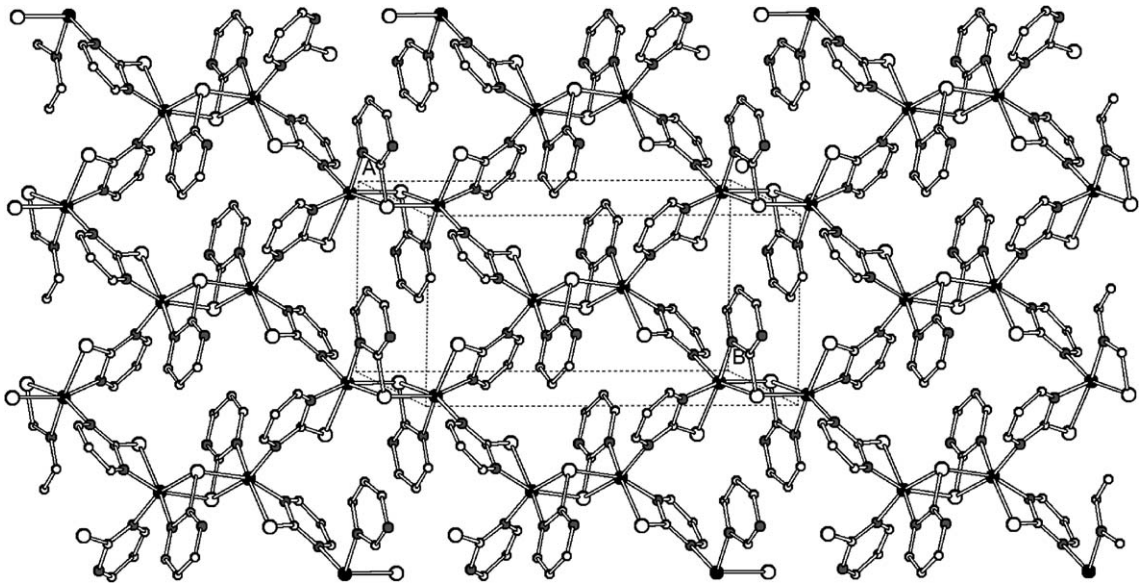

Fig. 18. The lamellar structure in compound $Ni_2(C_4N_2H_3S)_4$. Large white spheres: S; large black spheres: Ni; medium gray: N; small white: C.

well-known tetracyanoquinodimethane-based networks [42,46]. Of particular interest is that the use of thiolate ions to construct well-ordered and crystalline coordination networks has seen some remarkable success, in spite of the intractably low solubility generally associated with metal thiolate salts. The Chun group found that pyridinyl nitrogen-containing thiols could yield highly crystalline networks with ions such as Ag(I) [104] and even the transition metal ion Ni^{2+} [106]. For example, the coordination network with the formula $Ni_2(C_4N_2H_3S)_4$ with distinct electrical conductivity and ferromagnetic interaction between the nickel(II) centers was prepared by the hydrothermal reaction of $Ni(O_2CMe)_2$ with pyrimidine-2-thiol in a mixed solvent of DMF and H_2O. X-ray diffraction shows that the crystal structure possesses a lamellar structure formed from the conjugate system of pyrimidine rings and Ni^{2+} centers (see Figs. 18 and 19). Determination of the conductivity (powder sample from ground crystals) indicated an electrical conductivity of 5.00×10^{-3} S cm^{-1} at 28 °C which increased with temperature, indicating that $Ni_2(C_4N_2H_3S)_4$ was a semiconductor. From examining the crystal structure, the semiconducting property of $Ni_2(C_4N_2H_3S)_4$ was attributed to its characteristic structural feature of the interconnected array of nickel(II) with pyrimidine; the semiconducting property, on the other hand, provided evidence for nickel and pyridine ring interactions. Further exploration of thiolate ligand with other functional modifications may likely yield systems with wider range of crystalline structural features as well as solid state properties.

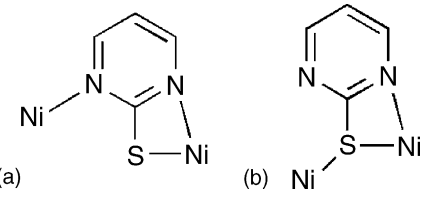

Fig. 19. (a and b) The coordination modes of pyrimidine-2-thiolate in compound $Ni_2(C_4N_2H_3S)_4$.

8. Conclusions

In addition to the traditional inorganic semiconductors and the currently pursued organic molecular semiconductors, coordination polymers could provide another class of compounds for the future development of functional semiconducting materials. The rich functionality arising from the interplay of organic and inorganic components in coordination polymers provides especially attractive potentials for their future applications as functional electronic materials. One major reason that coordination systems have been largely left out as semiconductive materials may be ascribed to the normally weak electronic coupling across coordination bonding units, which will likely result in poor charge transport behavior. Recent advances in the preparation of novel coordination compounds, as is reviewed above, may provide certain clues and suggestions for overcoming such electronic barriers in the eventual realization of effective semiconductive networks based on the coordination interactions. Further synthetic explorations of wider systems, as well as theoretical studies on the electronic structures and electronic device tests, should prove helpful for materializing this new class of compounds in the various practical applications. In a broader perspective, a number of outstanding problems and issues point to certain important future directions in this field, including: (1) further enhancement of coordination bonding strength for more efficient metal–ligand electronic coupling and better network stability, while, at the same time, maintaining the crystallinity of the solid state products; (2) combination of semiconductivity with other materials properties such as porosity, photoconductivity, magnetism and so on; (3) novel semiconductive properties such as multiple electronic band gaps and ambipolar transport behavior. The rich and flexible functionalities of the organic–inorganic systems of coordination polymers provide

great latitude and potential for resolving the problems encountered along these research directions.

References

[1] C.D. Dimitrakopoulos, P.R.L. Malenfant, Adv. Mater. 14 (2002) 99.
[2] H.E. Katz, Z. Bao, S.L. Gilat, Acc. Chem. Res. 34 (2001) 359.
[3] S.R. Forrest, Nature 428 (2004) 911.
[4] H.E. Katz, Z. Bao, J. Phys. Chem. B 104 (2000) 671.
[5] Z. Bao, Adv. Mater. 12 (2000) 227.
[6] D.M. Kaschak, S.A. Johnson, C.C. Waraksa, J. Pogue, T.E. Mallouk, Coord. Chem. Rev. 185–186 (1999) 403.
[7] E.H. Yonemoto, Y.I. Kim, R.H. Schmehl, J.O. Wallin, B.A. Shoulders, B.R. Richardson, J.F. Haw, T.E. Mallouk, J. Am. Chem. Soc. 116 (1994) 10557.
[8] A. Bose, P. He, C. Liu, B.D. Ellman, R.J. Twieg, S.D. Huang, J. Am. Chem. Soc. 124 (2002) 4.
[9] S. Nishimura, N. Abrams, B.A. Lewis, L.I. Halaoui, T.E. Mallouk, K.D. Benkstein, J. van de Lagemaat, A.J. Frank, J. Am. Chem. Soc. 125 (2003) 6306.
[10] A. Hagfeldt, M. Grätzel, Acc. Chem. Res. 33 (2000) 269.
[11] U. Bach, D. Lupo, P. Comte, J.E. Moser, F. Weissörtel, J. Salbeck, H. Spreitzer, M. Grätzel, Nature 395 (1998) 583.
[12] B. O'Regan, M. Grätzel, Nature 353 (1991) 737.
[13] G. Yu, J. Gao, J.C. Hummelen, F. Wudl, A.J. Heeger, Science 270 (1995) 1789.
[14] E.W. McFarland, J. Tang, Nature 421 (2003) 616.
[15] J. Xue, S. Uchida, B.P. Rand, S.R. Forrest, Appl. Phys. Lett. 84 (2004) 3013.
[16] P. Peumans, S. Uchida, S.R. Forrest, Nature 425 (2003) 158.
[17] A. Facchetti, Y. Deng, A. Wang, Y. Koide, H. Sirringhaus, T.J. Marks, R.H. Friend, Angew. Chem. Int. Ed. Engl. 39 (2000) 4547.
[18] M. Mushrush, A. Facchetti, M. Lefenfeld, H.E. Katz, T.J. Marks, J. Am. Chem. Soc. 125 (2003) 9414.
[19] A. Facchetti, M.-H. Yoon, C.L. Stern, H.E. Katz, T.J. Marks, Angew. Chem. Int. Ed. Engl. 42 (2003) 3900.
[20] H. Sirringhaus, P.J. Brown, R.H. Friend, M.M. Nielsen, K. Bechgaard, B.M.W. Langeveld-Voss, A.J.H. Spiering, R.A.J. Janssen, E.W. Meijer, P. Herwig, D.M. de Leeuw, Nature 401 (1999) 685.
[21] D.J. Gundlach, Y.Y. Lin, T.N. Jackson, D.G. Schlom, Appl. Phys. Lett. 71 (1997) 3853.
[22] H. Meng, M. Bendikov, G. Mitchell, R. Helgeson, F. Wudl, Z. Bao, T. Siegrist, C. Kloc, C.-H. Chen, Adv. Mater. 15 (2003) 1090.
[23] M.D. Watson, A. Fechtenkötter, K. Müllen, Chem. Rev. 101 (2001) 1267.
[24] C.D. Dimitrakopoulos, S. Purushothaman, J. Kymissis, A. Callegari, J.M. Shaw, Science 283 (1999) 822.
[25] A. Afzali, C.D. Dimitrakopoulos, T.L. Breen, J. Am. Chem. Soc. 124 (2002) 8812.
[26] A. Afzali, C.D. Dimitrakopoulos, T.O. Graham, Adv. Mater. 15 (2003) 2066.
[27] C.D. Sheraw, T.N. Jackson, D.L. Eaton, J.E. Anthony, Adv. Mater. 15 (2003) 2009.
[28] Q. Miao, T.-Q. Nguyen, T. Someya, G.B. Blanchet, C. Nuckolls, J. Am. Chem. Soc. 125 (2003) 10284.
[29] D.J. Gundlach, Y.Y. Lin, T.N. Jackson, S.F. Nelson, D.G. Schlom, IEEE Electron Device Lett. 18 (1997) 87.
[30] M. Shtein, J. Mapel, J.B. Benziger, S.R. Forrest, Appl. Phys. Lett. 81 (2002) 268.
[31] A.M. van de Craats, N. Stutzmann, O. Bunk, M.M. Nielsen, M. Watson, K. Müllen, H.D. Chanzy, H. Sirringhaus, R.H. Friend, Adv. Mater. 15 (2003) 495.
[32] M.G. Debije, J. Piris, M.P. De Haas, J.M. Warman, Z. Tomovic, C.D. Simpson, M.D. Watson, K. Müllen, J. Am. Chem. Soc. 126 (2004) 4641.
[33] J. Xue, S.R. Forrest, Appl. Phys. Lett. 79 (2001) 3714.
[34] N. Boden, R.J. Bushby, J. Clements, B. Movaghar, K.J. Fonobsn, T. Kreouzis, Phys. Rev. B: Condens. Matter 52 (1995) 13274.
[35] A.M. van de Craats, J.M. Warman, Adv. Mater. 13 (2001) 130.
[36] S.R. Batten, R. Robson, Angew. Chem. Int. Ed. Engl. 37 (1998) 1461.
[37] O.M. Yaghi, M. O'Keeffe, N.W. Ockwig, H.K. Chae, M. Eddaoudi, J. Kim, Nature 423 (2003) 705.
[38] C. Janiak, Dalton Trans. (2003) 2781.
[39] S.L. James, Chem. Soc. Rev. 32 (2003) 276.
[40] B. Kesanli, W. Lin, Coord. Chem. Rev. 246 (2003) 305.
[41] M. Hanack, S. Deger, A. Lange, Coord. Chem. Rev. 83 (1988) 115.
[42] R. Kato, Bull. Chem. Soc. Jpn. 73 (2000) 515.
[43] J.C. Zhong, Y. Misaki, M. Munakata, T. Kuroda-Sowa, M. Maekawa, Y. Suenaga, H. Konaka, Inorg. Chem. 40 (2001) 7096.
[44] M.B. Inoue, M. Inoue, M.A. Bruck, Q. Fernando, Chem. Commun. (1992) 515.
[45] X. Gan, M. Munakata, T. Kuroda-Sowa, M. Maekawa, Bull. Chem. Soc. Jpn. 67 (1994) 3009.
[46] A. Aumüller, P. Erk, G. Klebe, S. Hünig, J.U. von Schütz, H.-P. Werner, Angew. Chem. Int. Ed. Engl. 25 (1986) 740.
[47] R. Kato, H. Kobayashi, A. Kobayashi, J. Am. Chem. Soc. 111 (1989) 5224.
[48] R.A. Heintz, H.H. Zhao, O.Y. Xiang, G. Grandinetti, J. Cowen, K.R. Dunbar, Inorg. Chem. 38 (1999) 144.
[49] M. Munakata, L.P. Wu, G.L. Ning, Coord. Chem. Rev. 198 (2000) 171.
[50] E.L. Elliott, G.A. Hernandez, A. Linden, J.S. Siegel, Org. Biomol. Chem. 3 (2005) 407.
[51] M. Munakata, L.P. Wu, T. Kuroda-Sowa, M. Maekawa, Y. Suenaga, K. Sugimoto, Inorg. Chem. 36 (1997) 4903.
[52] S.Q. Liu, T. Kuroda-Sowa, H. Konaka, Y. Suenaga, M. Maekawa, T. Mizutani, G.L. Ning, M. Munakata, Inorg. Chem. 44 (2005) 1031.
[53] M. Munakata, L.P. Wu, T. Kuroda-Sowa, M. Maekawa, Y. Suenaga, G.L. Ning, T. Kojima, J. Am. Chem. Soc. 120 (1998) 8610.
[54] S.-L. Zheng, J.-P. Zhang, W.-T. Wong, X.-M. Chen, J. Am. Chem. Soc. 125 (2003) 6882.
[55] I.M. Vezzosi, A.F. Zanoli, L.P. Battaglia, A.B. Corradi, Dalton Trans. (1988) 191.
[56] A. Bondi, J. Phys. Chem. 68 (1964) 441.
[57] W. Frank, J. Schneider, S. Müller-Becker, Chem. Commun. (1993) 799.
[58] L.P. Battaglia, C. Bellitto, M.R. Cramarossa, I.M. Vezzosi, Inorg. Chem. 35 (1996) 2390.
[59] L.P. Battaglia, A. Bonamartini Corradi, I.M. Vezzosi, F.A. Zanoli, Dalton Trans. (1990) 1675.
[60] I.M. Vezzosi, L.P. Battaglia, A. Bonamartini Corradi, Dalton Trans. (1992) 375.
[61] M.B. Ferrari, M.R. Cramarossa, D. Iarossi, G. Pelosi, Inorg. Chem. 37 (1998) 5681.
[62] F.A. Cotton, E.V. Dikarev, M.A. Petrukhina, J. Am. Chem. Soc. 123 (2001) 11655.
[63] M.A. Petrukhina, K.W. Andreini, J. Mack, L.T. Scott, Angew. Chem. Int. Ed. Engl. 42 (2003) 3375.
[64] M.A. Petrukhina, K.W. Andreini, L. Peng, L.T. Scott, Angew. Chem. Int. Ed. Engl. 43 (2004) 5477.
[65] M.A. Petrukhina, L.T. Scott, Dalton Trans. (2005) 2969.
[66] B.W. Smucker, K.R. Dunbar, Dalton Trans. (2000) 1309.
[67] M. Fourmigué, C.E. Uzelmeier, K. Boubekeur, S.L. Bartley, K.R. Dunbar, J. Organomet. Chem. 529 (1997) 343.
[68] C.E. Uzelmeier, S.L. Bartley, M. Fourmigué, R. Rogers, G. Grandinetti, K.R. Dunbar, Inorg. Chem. 37 (1998) 6706.
[69] J.M. Asara, C.E. Uzelmeier, K.R. Dunbar, J. Allison, Inorg. Chem. 37 (1998) 1833.
[70] M. Munakata, T. Kuroda-Sowa, M. Maekawa, A. Hirota, S. Kitagawa, Inorg. Chem. 34 (1995) 2705.
[71] N. Avarvari, M. Fourmigué, Chem. Commun. (2004) 1300.
[72] E. Cerrada, C. Diaz, M.C. Diaz, M.B. Hursthouse, M. Laguna, M.E. Light, Dalton Trans. (2002) 1104.

[73] A.J. Barton, A.R.J. Genge, W. Levason, G. Reid, Dalton Trans. (2000) 2163.
[74] A.J. Barton, N.J. Hill, W. Levason, G. Reid, Dalton Trans. (2001) 1621.
[75] A.R.J. Genge, N.J. Hill, W. Levason, G. Reid, Dalton Trans. (2001) 1007.
[76] M.J. Hesford, N.J. Hill, W. Levason, G. Reid, J. Organomet. Chem. 689 (2004) 1006.
[77] N.J. Hill, W. Levason, G. Reid, A.J. Ward, J. Organomet. Chem. 642 (2002) 186.
[78] N.J. Hill, W. Levason, G. Reid, Inorg. Chem. 41 (2002) 2070.
[79] N.J. Hill, W. Levason, R. Patel, G. Reid, M. Webster, Dalton Trans. (2004) 980.
[80] W. Levason, N.J. Hill, G. Reid, Dalton Trans. (2002) 4316.
[81] Z. Xu, K. Li, J.C. Fettinger, J. Li, M.M. King, Cryst. Growth Des. 5 (2005) 423.
[82] K. Li, Z. Xu, H. Xu, J.M. Ryan, Chem. Mater. 17 (2005) 4426.
[83] K. Li, H. Xu, Z. Xu, M. Zeller, A.D. Hunter, Inorg. Chem. 44 (2005) 8855.
[84] J. Starbuck, N.C. Norman, A.G. Orpen, New J. Chem. 23 (1999) 969.
[85] N.W. Alcock, Adv. Inorg. Chem. Radiochem. 15 (1972) 1.
[86] J.D. Martin, K.B. Greenwood, Angew. Chem. Int. Ed. Engl. 36 (1997) 2072.
[87] J.D. Martin, B.R. Leafblad, Angew. Chem. Int. Ed. Engl. 37 (1998) 3318.
[88] J.D. Martin, R.F. Hess, P.D. Boyle, Inorg. Chem. 43 (2004) 3242.
[89] M. Julve, G. De Munno, G. Bruno, M. Verdaguer, Inorg. Chem. 27 (1988) 3160.
[90] M. Loï, E. Graf, M.W. Hosseini, A. De Cian, J. Fischer, Chem. Commun. (1999) 603.
[91] A. Neels, B.M. Neels, H. Stoeckli-Evans, A. Clearfield, D.M. Poojary, Inorg. Chem. 36 (1997) 3402.
[92] M. Ferigo, P. Bonhôte, W. Marty, H. Stoeckli-Evans, Dalton Trans. (1994) 1549.
[93] R.D. Rogers, A.H. Bond, J.L. Wolff, J. Coord. Chem. 29 (1993) 187.
[94] G.A. Bowmaker, J.M. Harrowfield, H. Miyamae, T.M. Shand, B.W. Skelton, A.A. Soudi, A.H. White, Aust. J. Chem. 49 (1996) 1089.
[95] J.M. Harrowfield, H. Miyamae, T.M. Shand, B.W. Skelton, A.A. Soudi, A.H. White, Aust. J. Chem. 49 (1996) 1043.
[96] C.Q. Xu, T. Kondo, H. Sakakura, K. Kumata, Y. Takahashi, R. Ito, Solid State Commun. 79 (1991) 245.
[97] C.R. Kagan, D.B. Mitzi, C.D. Dimitrakopoulos, Science 286 (1999) 945.
[98] D.B. Mitzi, Prog. Inorg. Chem. 48 (1999) 1.
[99] Z. Xu, D.B. Mitzi, Chem. Mater. 15 (2003) 3632.
[100] N. Zheng, X. Bu, P. Feng, J. Am. Chem. Soc. 124 (2002) 9688.
[101] J. Xie, X. Bu, N. Zheng, P. Feng, Chem. Commun. (2005) 4916.
[102] N. Zheng, X. Bu, H. Lu, L. Chen, P. Feng, J. Am. Chem. Soc. 127 (2005) 14990.
[103] J.P. Collman, J.T. McDevitt, G.T. Yee, M.B. Zisk, J.B. Torrance, W.A. Little, Synth. Met. 15 (1986) 129.
[104] W. Su, M. Hong, J. Weng, R. Cao, S. Lu, Angew. Chem. Int. Ed. Engl. 39 (2000) 2911.
[105] C.N.R. Rao, A. Ranganathan, V.R. Pedireddi, A.R. Raju, Chem. Commun. (2000) 39.
[106] Y. Zhao, M. Hong, Y. Liang, R. Cao, J. Weng, S. Lu, W. Li, Chem. Commun. (2001) 1020.